On Synchronization of Networks of Wilson-Cowan Oscillators with Diffusive Coupling

Saeed Ahmadizadeh[a], Dragan Nešić[a], Dean R. Freestone[b], David B. Grayden[a,b,c]

[a] *Department of Electrical and Electronic Engineering, The University of Melbourne, Parkville, VIC 3010, Australia*
[b] *Department of Medicine, St. Vincents Hospital, The University of Melbourne, Parkville, VIC, Australia*
[c] *Centre for Neural Engineering, The University of Melbourne, Parkville, VIC 3010, Australia*

Abstract

We investigate the problem of synchronization in a network of homogeneous Wilson-Cowan oscillators with diffusive coupling. Such networks can be used to model the behavior of populations of neurons in cortical tissue, referred to as neural mass models. A new approach is proposed to address conditions for local synchronization for this type of neural mass model. By analyzing the linearized model around a limit cycle, we study synchronization within a network with direct coupling. We use both analytical and numerical approaches to link the presence or absence of synchronized behavior to the location of eigenvalues of the Laplacian matrix. For the analytical part, we apply two-time scale averaging and the Chetaev theorem, while, for the remaining part, we use a recently proposed numerical approach. Sufficient conditions are established to highlight the effect of network topology on synchronous behavior when the interconnection is undirected. These conditions are utilized to address points that have been previously reported in the literature through simulations: synchronization might persist or vanish in the presence of perturbation in the interconnection gains. Simulation results confirm and illustrate our results.

Keywords: Wilson-Cowan oscillator, Synchronization, Complex network.

1. Introduction

Synchronization is a ubiquitous phenomenon observed in diverse networks of interconnected subsystems that arise in neuroscience, physics, biology, social networks, and many more. Synchronization occurs when the states or outputs of subsystems converge to the same behavior, and can be considered as the asymptotic stability of error vectors between the state (or output) vectors of two or more subsystems. Approaches for the study of synchronization can be categorized into two groups: global and local. Lipschitz [7], passivity [3], dissipativity [21], and semi-passivity [22] properties have been employed to study global synchronization. In these approaches, the subsystems in the network are required to satisfy a specific dissipation or passivity property. In some applications, it may be challenging to demonstrate that these properties are satisfied, and so local approaches are a useful alternative.

In local approaches, a linearization technique is utilized that indicates that synchronization in a network of oscillators can be analyzed via the well-known master stability equation (MSE) in which the eigenvalues of the Laplacian matrix play a crucial role [14]. In order to study the influence of interconnection gains on synchronization, the stability of the MSE has previously been evaluated using numerical approaches, which are computationally intensive. However, a possible way to reduce computational effort would be to combine analytical methods with numerical tools. In [26], synchronization of a network of oscillators with nonlinear dynamics was investigated analytically. Recently, Shafi et al. [20] proposed a framework to study synchronization in a network of oscillators by combining both analytical and numerical methods, allowing one to study the effects of interconnection gains on synchronization.

Synchronization of neural networks is thought to play a key role in information integration and processing. Synchronization of distributed brain regions has been speculated to play an important role in cognition [17]. Therefore, understanding the mechanisms that underpin synchrony in the brain is important. The Wilson-Cowan model [25] is of great interest since it is parsimonious, as it describes the activity of both excitatory and inhibitory populations of neurons and reproduces self-sustained oscillations observed in electroencephalography (EEG) signals. In particular, local synchronization of the Wilson-Cowan model has been investigated in the literature using the centre manifold theorem [11] and the notion of phase response curves [6]. These approaches only deal with weak coupling. However, synchronization can be observed in Wilson-Cowan networks with intermediate or strong coupling.

It is known that two factors have a significant impact on presence or absence of synchronization in the complex network: dynamical models of network nodes and network topology. In particular, investigating the effect of the latter has attracted much research and it is still an ongoing problem [4; 15]. More recently, this point has been explored in neuroscience using a computational model of the brain [23]. It has been observed that, in the network of oscillators, removing or adding interconnections between nodes can lead to the death or persistence of

Email addresses: s.ahmadizadeh@student.unimelb.edu.au (Saeed Ahmadizadeh), dnesic@unimelb.edu.au (Dragan Nešić), deanrf@unimelb.edu.au (Dean R. Freestone), grayden@unimelb.edu.au (David B. Grayden)

synchronous activity in the system. However, all these observations have been obtained only by simulations.

In this manuscript, we demonstrate that the framework of Shafi et al. [20] can be adapted to study local synchronization in a network of Wilson-Cowan oscillators with arbitrary coupling strengths. As far as we are aware, this is a new result. Our contribution is fourfold. First, the Wilson-Cowan model does not fit the general model considered in [14; 20; 26]. As a consequence, the analysis is different. Second, the Wilson-Cowan networks do not synchronize for all coupling gains. Therefore, we had to use an instability result for the linearized model based on the Chetaev theorem to develop a novel proof. This is different from the results in Shafi et al. [20], where local synchronization was shown for both weak and strong coupling. Furthermore, our results are also different from [26], where the authors presented a sufficient condition for synchronization that is conservative for our network. Third, we considered the directed coupling between oscillators in the network and our results are general. Fourth, we present sufficient conditions that relate the role of perturbations in the network topology, thereby explaining robustness and absence of synchronization.

The paper is organized as follow. In Section 2, we briefly introduce the Wilson-Cowan model of a single population as well as the network of such models with non-identical nodes. In Section 3, we formulate the problem for a more general network with identical nodes. In Section 4, the synchronization conditions are established for the network. Robustness of synchronization is analyzed in Section 5. Simulation results and conclusions are presented in Sections 6 and 7, respectively.

Notation. Throughout this paper, I_n denotes the identity matrix in $\mathbb{R}^{n\times n}$. The Kronecker product is denoted by $\otimes$. For a complex variable, vector or matrix, $\mathfrak{R}(\cdot)$ and $\mathfrak{I}(\cdot)$ stand for the real and imaginary parts. For a matrix $A \in \mathbb{R}^{N\times N}$, $\{\lambda_i(A)\}_{i=1}^N$ stands for ordered eigenvalues of matrix A such that $\lambda_{min} = \lambda_1$ and $\mathfrak{R}(\lambda_1) \leq \mathfrak{R}(\lambda_2) \leq \cdots \leq \mathfrak{R}(\lambda_N)$. The operator diag$(\cdot)$ constructs a block diagonal matrix from its arguments. $[A]_i$ denotes the i-th row of matrix $A \in \mathbb{R}^{N\times M}$.

2. Wilson-Cowan Model

Neural mass models describe the relationships between neural populations. Lumped parameter neural mass models are constructed by interconnecting neural populations that generate some realistic EEG patterns like alpha or beta waves. In this class of model, the dynamics of each neural population can be described by a linear first-order system coupled with a sigmoid non-linearity that converts the average membrane potential of a neural population into an average pulse density of action potentials. This model is given by

$$\dot{x}_s = -\alpha x_s + f(\rho + I), \tag{1}$$

where $x_s \in \mathbb{R}$ describes the average membrane potential of a single population that can be either excitatory x_E or inhibitory x_I. The parameter α is the population time constant and ρ denotes the sensory input or input from other neurons. The inputs from neighboring or distant populations are represented by I. $f_i : \mathbb{R} \to \mathbb{R}$ is a sigmoid function given by

$$f_i(\theta_j) = \frac{1}{1+\exp(-r_i\theta_j)} \quad , \quad r_i > 0,\ j = 1, 2. \tag{2}$$

The neural mass model of Wilson-Cowan [25] characterizes the behavior of spatially localized neural populations via a lumped parameter description. This model contains an excitatory and an inhibitory neural population that are coupled together and are considered as a single "node". The Wilson-Cowan model is described by

$$\dot{x}_i = -\Lambda_i x_i + F_i(\Upsilon_i + \Xi_i x_i + I_{x_i}), \tag{3}$$

where $x_i = [x_{E_i}, x_{I_i}]^T \in \mathbb{R}^2$ is a stack vector of the average membrane potentials of the excitatory and inhibitory populations, x_{E_i} and x_{I_i}, respectively. The vector $I_{x_i} = [I_{E_i}, I_{I_i}]^T \in \mathbb{R}^2$ represents the exogenous inputs that include the input from neighboring populations and/or external inputs such as controller inputs. The matrices $\Lambda_i, \Upsilon_i, \Xi_i$ are determined by

$$\Lambda_i = \begin{bmatrix} \alpha_{E_i} & 0 \\ 0 & \alpha_{I_i} \end{bmatrix} \quad , \quad \Upsilon_i = \begin{bmatrix} \rho_{x_{E_i}} \\ \rho_{x_{I_i}} \end{bmatrix} \quad , \quad \Xi_i = \begin{bmatrix} a_i & -b_i \\ c_i & -d_i \end{bmatrix}, \tag{4}$$

where a_i, b_i, c_i, d_i are positive constants and referred to as synaptic gains. The nonlinear function $F_i(\theta) : \mathbb{R}^2 \to \mathbb{R}^2$ is described by

$$F_i(\theta) = \left[f_i(\theta_1), f_i(\theta_2)\right]^T. \tag{5}$$

In order to interconnect Wilson-Cowan oscillators, it is assumed that the excitatory neural population of one node is coupled to the excitatory neural population of another node. The same coupling configuration is assumed for connection between inhibitory populations in two distinct nodes. In other words, if a node i is coupled to a node j with coupling gain w_{ij}, then the excitatory neural population and inhibitory neural population in node i are coupled to the excitatory and inhibitory neural populations in node j with the coupling gains w_{ij} and $-w_{ij}$, respectively. We note that this assumption is somewhat restrictive as these two interconnections can have different coupling gains in general [11; 24]. Although the interconnection between nodes was originally considered as a direct coupling, it has been proposed that diffusive coupling can be utilized to control oscillatory behaviors and, in particular, synchrony behavior of populations [24].

Now, consider a network with N Wilson-Cowan Oscillators interconnected with diffusive coupling. In this case, the dynamics of each node is represented by

$$\dot{x}_i = -\Lambda x_i + F_i\left(\Upsilon_i + \Xi_i x_i + D_s \sum_{j=1}^{N} w_{ij}(x_j - x_i)\right), \tag{6}$$

where $D_s = \text{diag}(1, -1)$ due to assuming the interconnections are restricted to being excitatory-excitatory and inhibitory-inhibitory .

3. Problem Formulation

In this section, we formulate the problem of synchronization in the network of Wilson-Cowan oscillators. It is worth mentioning that the Wilson-Cowan model (6) differs from the general model studied in [14; 20; 26]. In the Wilson-Cowan model, the nonlinearity term acts on the diffusive term $(x_i - x_j)$; however, in [14; 20; 26], the interactions between nodes have been considered as diffusion between nonlinear terms in the form of $f(x_i) - f(x_j)$. This fact leads to a different linearized model for the network of Wilson-Cowan oscillators compared to the linearized model in [14; 20; 26]. We interconnect more than two populations in (1) and consider a network of N homogeneous interconnected nodes in which every node is described by

$$\dot{x}_i = -\Lambda x_i + F\left(\Upsilon + \Xi x_i + D\sum_{j=1}^{N} w_{ij}(x_j - x_i)\right), \tag{7}$$

where $x_i \in \mathbb{R}^n$ is the state vector, $\Upsilon \in \mathbb{R}^n$ represents an external input applied to each node, and $\Xi \in \mathbb{R}^{n\times n}$ shows the internal coupling among states of the node. $F = (f, f, \ldots, f) : \mathbb{R}^n \to \mathbb{R}^n$ is a sufficiently smooth nonlinear function guaranteeing the existence of a solution. $D \in \mathbb{R}^{n\times n}$ is an arbitrary matrix, describing the inner coupling between states of all nodes. The interconnection between nodes and dynamics of each node are assumed to satisfy the following assumptions.

Assumption 1. *The interconnections among nodes are directed and there is no self loops. In this case, the interconnection topology is represented by a zero-sum row matrix $L \in \mathbb{R}^{\mathbb{N}\times\mathbb{N}}$, known as a graph Laplacian defined by $l_{ij} = -w_{ij}$ for $i \neq j$ and $l_{ii} = \sum_{j=1}^{N} w_{ij}$. We also assume that the interconnection graph has a spanning tree. In this case, the Laplacian matrix has exactly one zero eigenvalue $\lambda_1 = 0$, and other eigenvalues have positive real parts, i.e. $\Re(\lambda_k) > 0$ for $k = 2, \ldots, N$ [16].*

Assumption 2. *In the absence of interconnections, i.e. $w_{ij} = 0\ \forall i, j = 1, \ldots, N$, each node (7) has a periodic solution $\bar{x}(t) = \bar{x}(t + T)$ produced by an asymptotically stable limit cycle that satisfies*

$$\dot{\bar{x}} = -\Lambda\bar{x} + F\left(\Upsilon + \Xi\bar{x}\right). \tag{8}$$

The analysis that follows is based on the master stability function approach, where we linearize (7) around the oscillatory trajectory $\bar{x}(t)$. The linearized trajectory is given by

$$\begin{aligned}\dot{x}_i =& -\Lambda x_i + F\left(\Upsilon + \Xi\bar{x}\right)\\ &+ A(t)\left(\Xi\left(x_i - \bar{x}\right) + D\sum_{j=1}^{N} l_{ij}\left(x_j - x_i\right)\right),\end{aligned} \tag{9}$$

where $A(t) = \frac{\partial F}{\partial x}|_{\Upsilon+\Xi\bar{x}}$. Define $\tilde{x}_i = x_i - \bar{x}$, the difference between trajectories of each node and the oscillatory trajectory. Considering (8) and (9), the dynamics of $\tilde{x}_i$ can be expressed as

$$\dot{\tilde{x}}_i = -\Lambda\tilde{x}_i + A(t)\left(\Xi\tilde{x}_i + D\sum_{j=1}^{N} l_{ij}\left(\tilde{x}_j - \tilde{x}_i\right)\right), \tag{10}$$

which leads to the aggregated linearized system form as

$$\dot{\tilde{x}} = \left(I_N \otimes (-\Lambda + A(t)\Xi) - L \otimes A(t)D\right)\tilde{x}, \tag{11}$$

where $\tilde{x} = \mathrm{vec}(\tilde{x}_1, \ldots, \tilde{x}_N)$. Let Σ be the Jordan block associated with the Laplacian matrix, i.e. $L = U\Sigma U^{-1}$. Changing to new coordinates $\tilde{y} \in \mathbb{C}^{Nn}$, $\tilde{y} = (U^{-1} \otimes I_n)\tilde{x}$ gives

$$\dot{\tilde{y}} = \left(I_N \otimes (-\Lambda + A(t)\Xi) - \Sigma \otimes A(t)D\right)\tilde{y}. \tag{12}$$

Let us represent Σ as $\Sigma = \mathrm{diag}\{\Sigma_k\}_{k=1}^{p}$, where

$$\Sigma_k = \begin{bmatrix} \lambda_k & 1 & 0 & \ldots & 0\\ 0 & \lambda_k & 1 & \ldots & 0\\ 0 & 0 & \lambda_k & \ldots & 0\\ \vdots & \vdots & \ddots & \ddots & \vdots\\ 0 & 0 & 0 & \ldots & \lambda_k \end{bmatrix}_{m_k\times m_k}, \tag{13}$$

$\lambda_k(L) \in \mathbb{C}$ are eigenvalues of the Laplacian matrix, and $m_1 + \cdots + m_p = N$. Since Σ is a block diagonal matrix, (12) is decoupled into p independent systems described by

$$\dot{\tilde{y}}_k = \left(I_{m_k} \otimes (-\Lambda + A(t)\Xi) - \Sigma_k \otimes A(t)D\right)\tilde{y}_k\,, \quad k = 1, \ldots, p, \tag{14}$$

where $\tilde{y}_k \in \mathbb{C}^{m_k n}$, $\tilde{y}_k = [\tilde{y}_{k,1}^T, \ldots, \tilde{y}_{k,m_k}^T]^T$. Separating the real and imaginary part of $\tilde{y}_k$ in (14) leads to

$$\begin{aligned}\frac{d}{dt}\Re\left(\tilde{y}_k\right) =& \left(I_{m_k} \otimes (-\Lambda + A(t)\Xi) - \Re\left(\Sigma_k\right) \otimes A(t)D\right)\Re\left(\tilde{y}_k\right)\\ &+ \left(\Im\left(\Sigma_k\right) \otimes A(t)D\right)\Im\left(\tilde{y}_k\right)\\ \frac{d}{dt}\Im\left(\tilde{y}_k\right) =& \left(I_{m_k} \otimes (-\Lambda + A(t)\Xi) - \Re\left(\Sigma_k\right) \otimes A(t)D\right)\Im\left(\tilde{y}_k\right)\\ &- \left(\Im\left(\Sigma_k\right) \otimes A(t)D\right)\Re\left(\tilde{y}_k\right).\end{aligned} \tag{15}$$

Under Assumption 1, $\Sigma_1 = 0$. If (15) is asymptotically stable for $k = 2, \ldots, p$, then, according to Lemma 3 in [26], the underlying network becomes locally completely synchronized, i.e. $x_i(t) - x_j(t) \to 0, i, j = 1, \ldots, N$ for some initial condition. Hence, in the rest of the paper, we investigate the asymptotic stability or instability of the system (15). The following lemma states that this can be done by analyzing the interconnected systems that have lower dimension than (15).

Lemma 1. *Consider the dynamical system described in (15) and the corresponding interconnected system as*

$$\begin{aligned}\dot{\zeta}_{1k} &= \left((-\Lambda + A(t)\Xi) - \beta_{R_k}A(t)D\right)\zeta_{1k} + \beta_{I_k}A(t)D\zeta_{2k}\\ \dot{\zeta}_{2k} &= \left((-\Lambda + A(t)\Xi) - \beta_{R_k}A(t)D\right)\zeta_{2k} - \beta_{I_k}A(t)D\zeta_{1k}\end{aligned} \tag{16}$$

where β_{R_k} and β_{I_k} are the real and imaginary parts of λ_k respectively. If (16) is asymptotically stable (unstable), then (15) is asymptotically stable (unstable).

Proof. See Appendix A.

4. Stability Analysis of the Linearized Model

According to the discussion in the previous section and Lemma 1, presence/absence of local synchronization is directly

related to stability/instability of the linearized system (16), which in turn depends on the real and imaginary parts. Without loss of generality, we assume that β_{I_k} is non-negative, since stability or instability of (16) are invariant with respect to the sign of β_{I_k}. In order to simplify the presentation, the subscript k is dropped. We find it convenient to divide the parameter space into three regions and, for each region, we have proven different stability properties using different analysis method. Therefore, we divide the parameter space $\Omega_\beta = \{(\beta_R, \beta_I) \mid \beta_R > 0,\ \beta_I \geq 0\}$ into three regions: $\Omega^1_\beta = \{(\beta_R, \beta_I) \mid 0 < \beta_R \leq \beta_{R_{min}},\ 0 \leq \beta_I \leq \psi(\beta_R)\}$ with $\psi : [0, \beta_{R_{min}}] \to \mathbb{R}_{\geq 0}$, $\Omega^2_\beta = \{(\beta_R, \beta_I) \mid \beta_R \geq \beta_{R_{max}},\ 0 \leq \beta_I \leq \infty\}$, $\Omega^3_\beta = \{(\beta_R, \beta_I) \in \Omega_\beta - \{\Omega_1 \cup \Omega_2\}\}$.

For the first region Ω^1_β, we present Proposition 1 and Proposition 2 to check instability and stability of the linearized model (16). The value of $\beta_{R_{min}}$ and function $\psi(\beta_R)$ are also specified in these propositions. Proposition 1 is a result of Lemma A.2 in Appendix A. For $\beta_I = 0$, this lemma presents an instability condition using two-time scale averaging that can be used to develop a counterpart instability result of Proposition 3.1 of Shafi et al. [20]. In Proposition 3, we show that there exists $\beta_{R_{max}}$ such that (16) always becomes unstable in the region Ω^2_β. In Section 4.2, we present a numerical approach for parameter space Ω^3_β that follows ideas from robust control [20].

4.1. Synchronization in Set Ω^1_β

In the set Ω^1_β, we used the two-time scale averaging method following the similar idea of [20]; however, our result differs due to an extra term $A(t)$ appearing in the interconnection terms in (16). If $\beta_R = \beta_I = 0$, (16) is decomposed as two independent systems with the same dynamics:

$$\dot{\zeta}_i = (-\Lambda + A(t)\Xi)\,\zeta_i, \tag{17}$$

for $i = 1, 2$. In this case, due to Assumption 2, (17) has a T-periodic solution that is associated with a stable limit cycle in the original system (8). We denote $\phi_i(t, t_0)$ the principle state transition matrix of periodic dynamics (17) for $i = 1, 2$. Since both systems have the same dynamics, we have $\phi_1(t, t_0) = \phi_2(t, t_0) = \phi(t, t_0)$. The Floquet theory [9] indicates that the $\phi(t, t_0)$ is a T-periodic matrix that can be written as

$$\phi(t, t_0) = S(t) \exp\left(H\,(t - t_0)\right) R(t_0)\,, \tag{18}$$

where $S(t)$ is also a T-periodic matrix and $R(t) = S^{-1}(t)$. The columns of S denoted by s_i and rows of $R(t)$ denoted by r_j^T are orthonormal, $r_j^T s_i = \delta_{ij}$. The matrix H is known as the *monodromy matrix*, which satisfies $\phi(t_0 + T, t_0) = J \exp(HT)\, J^{-1}$ and J is a matrix that contains eigenvectors of $\phi(t_0 + T, t_0)$. For a stable limit cycle, the monodromy matrix H has the structure $H = \mathrm{diag}(0, H_2)$, where H_2 is an $(n-1) \times (n-1)$ Hurwitz matrix that contains non-zero Floquet exponents. Even though computing the analytical forms of $\phi(t, t_0)$, H_2, $S(t)$, and $R(t)$ is typically impossible, there are effective approaches that can be used to compute the matrices numerically. For example, an approach was proposed by Demir et al. [8]. Floquet theory implies that the change of coordinate $[s_i^T, r_i^T]^T = R(t)\zeta_i$ transforms (16) to the representation

$$\begin{bmatrix} \dot{s}_i \\ \dot{r}_i \end{bmatrix} = (H - \beta_R R(t) A(t) D S(t)) \begin{bmatrix} s_i \\ r_i \end{bmatrix} - (-1)^i \beta_I R(t) A(t) D S(t) \begin{bmatrix} s_{3-i} \\ r_{3-i} \end{bmatrix}, \tag{19}$$

for $i = 1, 2$. For small values of β_R, analysis of stability of (19) can be conducted using a two-time scale averaging method.

Next, we use Proposition 1 to demonstrate an instability condition of (19), and then Proposition 2 to provide sufficient conditions for asymptotic stability of (19).

Proposition 1. ***(Instability with Weak Coupling)*** *Let r_1^T and s_1 be the first row and column of $R(t)$ and $S(t)$ in (18), respectively. For a given matrix D, if*

$$\int_0^T r_1^T(\tau) A(\tau) D s_1(\tau) d\tau < 0, \tag{20}$$

there exist $\beta_{R_{min}}$ and $\psi : [0, \beta_{R_{min}}] \to \mathbb{R}_{\geq 0}$ so that

$$\begin{aligned} \dot{\zeta}_1 &= ((-\Lambda + A(t)\Xi) - \beta_R A(t) D)\,\zeta_1 + \beta_I A(t) D \zeta_2 \\ \dot{\zeta}_2 &= ((-\Lambda + A(t)\Xi) - \beta_R A(t) D)\,\zeta_2 - \beta_I A(t) D \zeta_1 \end{aligned} \tag{21}$$

is unstable for every $\beta_R \in (0, \beta_{R_{min}}]$ and the corresponding $\beta_I \in [0, \psi(\beta_R)]$. The value of $\beta_{R_{min}}$ and function $\psi(.)$ can be obtained from Lemma 2.

Proof. Proposition 1 is proven by applying Lemma 2 (see Appendix A) to the system (19). □

Proposition 2. ***(Stability with Weak Coupling)*** *Let r_1^T and s_1 be the first row and column of $R(t)$ and $S(t)$ in (18), respectively. For a given matrix D, if*

$$\int_0^T r_1^T(\tau) A(\tau) D s_1(\tau) d\tau > 0, \tag{22}$$

there exist $\beta_{R_{min}}$ and $\psi : [0, \beta_{R_{min}}] \to \mathbb{R}_{\geq 0}$ so that system (21) is asymptotically stable for every $\beta_R \in (0, \beta_{R_{min}}]$ and the corresponding $\beta_I \in [0, \psi(\beta_R)]$. Furthermore, decompose matrix $A(t)D$ with dimensions consistent with the monodromy matrix so that

$$A(t)D = \begin{bmatrix} \urcorner_{11}(t) & \urcorner_{12}(t) \\ \urcorner_{21}(t) & \urcorner_{22}(t) \end{bmatrix}.$$

Assume that there exists $\iota_{ij} > 0$ such that $\|\urcorner_{ii}(t)\| \leq \iota_{ij}$ for all $t \geq 0$. Then

$$\beta_{R_{min}} = \min\{\epsilon_1, \epsilon_2, \epsilon_3\},$$

where $\epsilon_1 = \frac{1}{2T\iota_{11}}$, $\epsilon_2 = \frac{1}{\iota_{22}}$, and ϵ_3 satisfies the following inequality,

$$\mathcal{X}(\epsilon_3) = \begin{bmatrix} \mathcal{X}_{11} & \mathcal{X}_{12} \\ \mathcal{X}_{12} & \mathcal{X}_{22} \end{bmatrix} < 0,$$

with $\mathcal{X}_{11} = -(\epsilon_3\gamma - 2\epsilon_3^2\gamma T\iota_{11})$, $\mathcal{X}_{22} = -(1 - \epsilon_3\iota_{22})$, $\mathcal{X}_{12} = \frac{1}{2}(\epsilon_3\gamma\iota_{12} + \epsilon_3\iota_{21} + \epsilon_3^2(2T\iota_{21}\iota_{11}))^2$, and $\gamma = \frac{1}{1-2\epsilon_1 T\iota_{11}}$. Now, for every $\beta_R \in (0, \beta_{R_{min}}]$, the corresponding value $\psi(\beta_R)$ is obtained by solving the following optimization problem,

$$\psi(\beta_R) = \max_{\bar{\beta} > 0} \bar{\beta} \qquad s.t. \quad \begin{bmatrix} \mathcal{X}(\beta_R) & \bar{\beta}\mathcal{Z}(\beta_R) \\ \bar{\beta}\mathcal{Z}(\beta_R) & \mathcal{X}(\beta_R) \end{bmatrix} < 0, \tag{23}$$

with $\mathcal{Z}(\beta_R) = \begin{bmatrix} \gamma\iota_{11}(1 + 2T\beta_R\iota_{11}) & \gamma\iota_{12} \\ (1 + 2T\beta_R\iota_{11})\iota_{21} & \iota_{22} \end{bmatrix}$.

Proof. Proposition 2 can be proven by using the same technique in Lemma A.1 in Shafi et al. [20] and following the same argument in Lemma 1 in Appendix A to the system (19). □

Propositions 1 and 2 demonstrate that if the system is unstable (or asymptotically stable) with $\beta_I = 0$, then it stays unstable (or asymptotically stable) with sufficiently small β_I. In this case, one needs to solve the optimization problem presented in the proof of Lemma 2 in Appendix A or in (23) for every $\beta_R \in (0, \beta_{R_{min}}]$, which itself is a computational approach. It is worth mentioning that this approach is not as computationally expensive as the numerical approach presented in the section 4.2. In addition, these two propositions are powerful tools when we know that β_I is zero; for instance, in the undirected case. We refer the interested reader to [2] for the undirected case.

Remark 1. *For the Wilson-Cowan model, the matrix $A(t) \in \mathbb{R}^{2\times 2}$ has the structure*

$$A(t) = \begin{bmatrix} \frac{\partial F}{\partial \theta}|_{\theta=[\Upsilon+\Xi\bar{x}]_1} & 0 \\ 0 & \frac{\partial F}{\partial \theta}|_{\theta=[\Upsilon+\Xi\bar{x}]_2} \end{bmatrix}. \tag{24}$$

Considering the structure of matrix D, condition (20) in Proposition 1 can be written as

$$\int_0^T (r_{11}(\tau)A_{11}(\tau)w_{11}(\tau) - r_{12}(\tau)A_{22}(\tau)w_{21}(\tau))d\tau < 0, \tag{25}$$

and condition (22) of Proposition 2 can be written as

$$\int_0^T (r_{11}(\tau)A_{11}(\tau)w_{11}(\tau) - r_{12}(\tau)A_{22}(\tau)w_{21}(\tau))d\tau > 0. \tag{26}$$

Furthermore, an alternative choice for matrix $\mathcal{Z}$ in Proposition 2 is

$$\mathcal{Z}(\beta_R) = \begin{bmatrix} 0 & \gamma\iota_{12} \\ (1 + 2T\beta_R\iota_{11})\iota_{21} & 0 \end{bmatrix}.$$

4.2. Synchronization in Set Ω^3_β

In this subsection, we study stability of (16) for $\beta_R \in [\beta_{R_{min}}, \beta_{R_{max}}]$ and $\beta_I \in [0, \infty]$ by adopting a numerical approach proposed by [20]. We represent the matrices $\beta_R D$ and $\beta_I D$ as

$$\beta_R D = M_1 + B_1\Delta_1 C_1 \quad , \quad \beta_I D = M_2 + B_2\Delta_2 C_2, \tag{27}$$

where $M_i \in \mathbb{R}^{n\times n}, B_i \in \mathbb{R}^{n\times m}, C_i \in \mathbb{R}^{m\times n}$, and $\Delta_i \in \mathbb{R}^{m\times m}$ are diagonal matrices whose diagonal entries vary in $[-1, 1]$ for $i = 1, 2$. It should be noted that the matrices in (27) are chosen in the way that, by varying the matrices Δ_1 and Δ_2, the right side of (27) generates all matrices $\beta_R D$ and $\beta_I D$ that are obtained by varying β_R and β_I respectively. Then, the system (16) can be written as a linear periodic time-varying system with block uncertainty $\Delta = \text{diag}(\Delta_1, \Delta_1, \Delta_2, \Delta_2)$:

$$\dot{\tilde{\zeta}} = \bar{A}(t)\tilde{\zeta} + \bar{B}(t)q \quad , \quad z = \bar{C}\tilde{\zeta} \quad , \quad q = \Delta z, \tag{28}$$

where

$$\begin{aligned} \bar{A}(t) &= \begin{bmatrix} -\Lambda I + A(t)\Xi - A(t)M_1 & A(t)M_2 \\ -A(t)M_2 & -\Lambda I + A(t)\Xi - A(t)M_1 \end{bmatrix} \\ \bar{B}(t) &= \begin{bmatrix} -A(t)B_1 & 0 & A(t)B_2 & 0 \\ 0 & -A(t)B_1 & 0 & -A(t)B_2 \end{bmatrix} \\ \bar{C} &= \begin{bmatrix} C_1^T & 0 & 0 & C_2^T \\ 0 & C_1^T & C_2^T & 0 \end{bmatrix}^T, \end{aligned} \tag{29}$$

with $\tilde{\zeta} = [\zeta_1^T, \zeta_2^T]^T \in \mathbb{R}^{2n}$, and $z \in \mathbb{R}^{2m}$ and $q \in \mathbb{R}^{4m}$ are outputs of the linear periodic time-varying system and uncertainty block. In order to check stability of (28), structured singular value (SSV) analysis is performed on a truncated harmonic state space model of (28). Under the assumption that $\bar{A}(t), \bar{B}(t)$ are continuous functions of t, using Fourier series, the state space model (28) can be represented in the form of a harmonic state space model

$$sY = (\bar{\mathcal{A}} - \mathcal{N})Y + \bar{\mathcal{B}}Q \quad , \quad Z = CY \quad , \quad Q = \tilde{\Delta}Y, \tag{30}$$

where $\bar{\mathcal{A}}, \mathcal{N}, \bar{\mathcal{B}}$ are infinite-dimensional matrices with complex entries. We refer to Shafi et al. [20] and Zhou and Hagiwara [27] for further details on such a harmonic state space model.

Although the harmonic state space model (30) is an infinite dimensional model, it can be approximated with a truncated model that considers the dominant harmonics in the Fourier series of $\tilde{\zeta}(t)$ [18]. Once the truncated model of (30) is computed, the structured singular value (SSV) μ can be calculated using a numerical approach such as *mussv* in the Robust Control Toolbox. It is difficult to compute SSV by considering all possible combinations of β_R and β_I, since β_I varies up to infinity. However, if the number of nodes in the network is fixed, Proposition 1 in [1] states that imaginary parts of an N-dimensional Laplacian matrix satisfy $\|\beta_I\| \leq \|\beta_R\| \cot \frac{\pi}{N}$. In this case, we can split the space into several segments and run the computational approach in every segment. If $\mu \leq 1$, (15) is stable for all values of β_R and β_I in that segment. If $\mu > 1$, we can compute the matrix Δ with the smallest norm that leads to instability of (15). It is worth mentioning that the matrices in (27) cover all possible coupling strengths for the intermediate coupling.

Remark 2. *As stated in [20], the proposed numerical approach leads to less conservative results than other numerical methods such as lifting approach or computation of Lyapunov exponent. For large values of β_I, our numerical experiences show that the mussv function faces a convergence issue, which results from singularity of matrices in computing singular value decomposition. For those values of β_I, we checked the stability of (15) by computing the Lyapunov exponent [14].*

4.3. Synchronization in Ω^2_β

As mentioned earlier, the results of this subsection are derived for the network of Wilson-Cowan oscillators. We present a property about $f(\theta)$ that turns out to be crucial in the proof of Proposition 3.

Fact 1. *The sigmoid function $f(\theta)$ (2) is a continuous function with positive and bounded derivative, i.e. $0 \leq f_{min} \leq f_\theta(\theta) \leq f_{max}$ for all $\theta \in \mathbb{R}$. In addition, $f_\theta(\theta) \to 0$ iff $\theta \to \pm\infty$.*

Proposition 3. ***(Instability with Strong Coupling for the Wilson-Cowan Model)*** *Consider the dynamical system described by the state space model*

$$\begin{aligned}\dot{\zeta}_1 &= ((-\Lambda + A(t)\Xi) - \beta_R A(t) D)\,\zeta_1 + \beta_I A(t) D \zeta_2 \\ \dot{\zeta}_2 &= ((-\Lambda + A(t)\Xi) - \beta_R A(t) D)\,\zeta_2 - \beta_I A(t) D \zeta_1,\end{aligned} \tag{31}$$

where Λ, Ξ, D are given by (4) and $A(t)$ is computed from linearization of F (5) around the limit cycle. Then, there exists a positive scalar ϵ^* such that (31) is unstable for every $\beta_R \geq \beta_R^*$ and for every $\beta_I \in \mathbb{R}$. Furthermore, $\beta_R^* = \max\{a, d, \beta_{R_1}\}$ and β_{R_1} can be obtained from the following optimization problem:

$$\begin{aligned}&\beta_{R_1} = \min_{\beta>0} \beta \\ &s.t. \quad \begin{bmatrix} \alpha_E + (\beta - a)\underline{\mathfrak{A}}_{11} & -\frac{1}{2}(|b|\overline{\mathfrak{A}}_{11} + |c|\overline{\mathfrak{A}}_{22}) \\ -\frac{1}{2}(|b|\overline{\mathfrak{A}}_{11} + |c|\overline{\mathfrak{A}}_{22}) & -\alpha_I + (\beta - d)\underline{\mathfrak{A}}_{22} \end{bmatrix} > 0,\end{aligned} \tag{32}$$

where $0 < \underline{\mathfrak{A}}_{ii} \leq A_{ii}(t) \leq \overline{\mathfrak{A}}_{ii}$, $i = 1, 2$ for all $t \geq 0$.

Proof. For the Wilson-Cowan model, the matrix $A(t) \in \mathbb{R}^{2\times 2}$ is a diagonal matrix that is given by (24). Due to Fact 1, there exists a non-zero positive scalar $\underline{\mathfrak{A}}_{ii}, \overline{\mathfrak{A}}_{ii}$ such that $0 < \underline{\mathfrak{A}}_{ii} \leq A_{ii}(t) \leq \overline{\mathfrak{A}}_{ii}$, $i = 1, 2$ for all $t \geq 0$. Now, consider a candidate Lyapunov function $V(\zeta_1, \zeta_2) = \sum_{i=1}^{2} \frac{1}{2}(\zeta_{i,2}^2 - \zeta_{i,1}^2)$ with $\zeta_i = [\zeta_{i,1}, \zeta_{i,2}]^T$. Taking the derivative along (31) leads to

$$\begin{aligned}\dot{V} = \sum_{i=1}^{2} \Big(&(-\alpha_I + (\beta_R - d)\, A_{22}(t))\, \zeta_{i,2}^2 + (cA_{22}(t) + bA_{11}(t))\, \zeta_{i,1}\zeta_{i,2} \\ &- (-\alpha_E + (a - \beta_R)\, A_{11}(t))\, \zeta_{i,1}^2 \Big).\end{aligned} \tag{33}$$

If $\beta_R \geq \max\{a, d\}$, then

$$\begin{aligned}\dot{V} \geq \sum_{i=1}^{2} &(-\alpha_I + (\epsilon - d)\underline{\mathfrak{A}}_{22})|\zeta_{i,2}|^2 + (\alpha_E + (\epsilon - a)\underline{\mathfrak{A}}_{11})|\zeta_{i,1}|^2 \\ &- (|c|\overline{\mathfrak{A}}_{22} + |b|\overline{\mathfrak{A}}_{11})|\zeta_{i,1}||\zeta_{i,2}| \,.\end{aligned} \tag{34}$$

For large values of ϵ, the first and second terms of (34) are positive and hence $\dot{V}$ is positive. If (32) holds, then $\dot{V} > 0$. Note that the set $\Omega \triangleq \{(\zeta_1, \zeta_2) \in \mathbb{R}^4 \mid V \geq 0\}$ is nonempty, since the candidate Lyapunov function is quadratic type. Hence, according to Chetaev's theorem for time-varying systems [10], the origin of (31) is unstable. This completes the proof. □

5. Network Topology and Synchronization

In this section, we aim to address robustness of synchronization with respect to the perturbation in the interconnection gains between nodes. We restrict our analysis to a network of Wilson-Cowan oscillators with N nodes and undirected interconnection. In this case, (16) is decomposed to two identical and independent systems and, therefore, the synchronization of the network is determined by $\dot{\zeta}_1 = ((-\Lambda + A(t)\Xi) - \beta_R A(t) D)\,\zeta_1$. We assume the eigenvalues of Laplacian matrix L satisfy

$$\{\lambda_k(L)\}_{k=2}^{N} \in (\beta_{R_{min}}, \beta_{R_{max}}), \tag{35}$$

where $(\beta_{R_{min}}, \beta_{R_{max}})$ is the largest interval for which the initial network is synchronized. The interconnection gains of the original network are perturbed and the associated Laplacian matrix is denoted by L_Δ. In this case, the Laplacian matrix of the perturbed network, referred as the "perturbed Laplacian matrix", can be written as

$$L_\Delta = L + \Delta L, \tag{36}$$

where ΔL is a "Laplacian-like" matrix, which is symmetric and zero row sum but not necessarily positive definite. The question is to find conditions on perturbations that lead to the presence or absence of synchronous behavior in the perturbed network.

Proposition 4 guarantees the persistence of synchronous behavior for a class of perturbations that satisfies (37). However, it does not determine the effects of perturbations that violate the condition, since that perturbations can either maintain the eigenvalues in the interval $[\beta_{R_{min}}, \beta_{R_{max}}]$ or take at least one eigenvalue out of this interval. To the best of our knowledge, there is no available result that answers this case in general. Proposition 5 presents conditions that ensure absence of synchronous behavior in the perturbed network.

Proposition 4. *Consider a network of Wilson-Cowan oscillators with N nodes and the corresponding Laplacian matrix L. Furthermore, assume the eigenvalues of L satisfy (35). If the following inequality holds,*

$$\begin{aligned}\max\{|\lambda_N(\Delta L)|, |\lambda_1(\Delta L)|\} \leq \\ \min\Big\{\lambda_2(L) - \beta_{R_{min}}, \beta_{R_{max}} - \lambda_n(L)\Big\},\end{aligned} \tag{37}$$

the perturbed network also shows synchronous behavior similar to unperturbed network.

Proof. Using Weyl's inequality [5], the eigenvalues of perturbed Laplacian matrix L_Δ satisfy $\lambda_1(\Delta L) \leq \lambda_k(L_\Delta) - \lambda_k(L) \leq \lambda_N(\Delta L)$ for $k = 1, \ldots, N$. Condition (37) ensures that $\lambda_2(L_\Delta)$, $\lambda_N(L_\Delta)$ stay in the interval $(\beta_{R_{min}}, \beta_{R_{max}})$, which implies that the synchronization persists in the presence of perturbation. □

Proposition 5. *Consider a network of Wilson-Cowan oscillators with N nodes and the corresponding Laplacian matrix L. Furthermore, assume the eigenvalues of L satisfy (35). If one of the following inequalities holds,*

$$\min_{j=1,2}\{\lambda_{2+j}(L) + \lambda_{2-j}(\Delta L)\} < \beta_{R_{min}}, \tag{38}$$

$$\max_{j=1,\ldots,n}\{\lambda_{n-j+1}(L) + \lambda_j(\Delta L)\} > \beta_{R_{max}}, \tag{39}$$

the synchronous behavior disappears in the perturbed network.

Proof. Considering (36) and Weyl's inequality [5], we have

$$\lambda_2(L_\Delta) \leq \min_{j=1,2}\{\lambda_{2+j}(L) + \lambda_{2-j}(\Delta L)\} \tag{40}$$

$$\lambda_n(L_\Delta) \geq \max_{j=1,\ldots,n}\{\lambda_{n-j+1}(L) + \lambda_j(\Delta L)\}. \tag{41}$$

If the right side of (40) is smaller than $\beta_{R_{min}}$, $\lambda_2(L_\Delta)$ is located outside of interval $[\beta_{R_{min}}, \beta_{R_{max}}]$, which means that synchronization vanishes in the network. Similarly, if the right side of (41) is larger than $\beta_{R_{max}}$, the network becomes desynchronized. □

Remark 3. *Conditions in Propositions 4 and 5 can be numerically verified if the Laplacian-like matrix ΔL is known. It is hard to express eigenvalues of ΔL in terms of perturbation terms in interconnection gains; however, for some simple cases, this is possible. As an example, consider the case where an arbitrary two nodes i and i' with corresponding interconnection gain $l_{ii'}$ is perturbed by $\delta l_{ii'}$. It is straightforward to check that the Laplacian-like matirx ΔL has $n-1$ zero eigenvalues and a non-zero eigenvalues $2\delta l_{ii'}$. For this case, condition (37) is simplified to*

$$|\delta l_{ii'}| \leq \min\left\{\frac{\lambda_2(L) - \beta_{R_{min}}}{2}, \frac{\beta_{R_{max}} - \lambda_N(L)}{2}\right\}. \tag{42}$$

The conditions (38) and (39) are also simplified to

$$\delta l_{ii'} < \frac{\beta_{R_{min}} - \lambda_3(L)}{2}, \tag{43}$$

$$\delta l_{ii'} > \frac{\beta_{R_{max}}}{2}. \tag{44}$$

6. Simulation Results

In this section, we present simulation results to validate the proposed approach to study of synchronization in a network of Wilson-Cowan oscillators. The Wilson-Cowan model exhibits oscillatory behavior resulting from the existence of a stable limit cycle that appears from the Andronov-Hopf-bifurcation of equilibrium point [11]. In the simulations, we choose the following set of variables that guarantees oscillatory behavior: $a = 10,\ b = 10,\ c = 10,\ d = -2,\ \rho_x = 2,\ \rho_y = -6$.

To analyze the network, we first compute the matrix $A(t)$ in (15) using the oscillatory behavior of each node. In the next step, we study the effect of weak coupling on stability of (15). We then check condition (20) in Proposition 1 and (22) in Proposition 2 using the numerical approach. For a Wilson-Cowan model, the instability condition holds. This means that there exists an $\beta_{R_{min}}$ such that, for every interconnection gain smaller than this value, (15) is unstable when $\beta_I = 0$. The value of $\beta_{R_{min}}$ is computed from the proof of Lemma 2 in Appendix A. In our case, $\beta_{R_{min}} = 0.034$. We then follow the approach stated in Proposition 1 to find the region Ω^1_β in which the system is unstable. In the next step, we apply Proposition 3 to find the minimum value of $\beta_{R_{max}}$ such that, for every $\beta_R \geq \beta_{R_{max}}$, (15) is unstable irrespective of the value of β_I. Following the proof of the proposition, we obtain $\beta_{R_{max}} = 15$, which means that $\Omega^2_\beta = \{(\beta_R, \beta_I)\,|\,\beta_R \geq 15,\ 0 \leq \beta_I \leq \infty\}$. Then, the computational algorithm in Section 4.2 is exploited in the space Ω^3_β. Note that the matrices $\beta_R D$ and $\beta_I D$ can be written in the form of (27) using $M_i = \text{diag}\left(\frac{\beta_{R_{max}}+\beta_{R_{min}}}{2}, -\frac{\beta_{R_{max}}+\beta_{R_{min}}}{2}\right)$, $B_i = \text{diag}\left(\frac{\beta_{R_{max}}-\beta_{R_{min}}}{2}, \frac{\beta_{R_{max}}-\beta_{R_{min}}}{2}\right)$, $\Delta_i = \text{diag}(\delta_i, \delta_i)$ and $C_i = \text{diag}(1, -1)$ for $i = 1, 2$.

The first fifteen harmonics of the Fourier series are sufficient to approximate the oscillatory trajectories in order to find the truncated harmonic state space model. To reduce numerical computation errors, we split the space Ω^2_β into some subspaces and follow the computational approach. As pointed out in Remark 2, we checked the stability or instability of the system via computing the Lyapunov exponent for large values of β_I. The computational results reveal that the system (15) is stable for all $\beta_R \in [5, 15]$ when $\beta_I = 0$.

The stability/instability region for the system (15) is depicted in Figure 1. This figure indicates that when the real parts of the eigenvalues are small, the system seems to be unstable irrespective of the values of imaginary parts; however, Proposition 1 states that for small values of real parts, there is a region in which the system is unstable. It is an open problem to analytically show whether this is true or not in general. This figure also shows that, in the interval $\beta_R \in [9.4, 15)$, the system is stable as long as β_I is very small. For the intermediate values of β_R, the stability of system behaves in different ways as β_I increases. In the intervals $\beta_R \in [2, 6.4)$, the system is unstable for small values of β_I, becomes stable and then unstable as β_I increases. For the interval $\beta_R \in [4, 6.5) \cup (7.69]$, it is stable for β_I small. Then it becomes unstable, stable (in small interval for β_I), and finally unstable by changing β_I. In the interval $\beta_R \in [6.5, 7.6]$, the system stays stable as long as the values of β_I becomes sufficiently large.

To verify this observation, we consider a network of Wilson-Cowan models with five nodes illustrated in Figure 2 (a). The Laplacian matrix has five eigenvalues, $\lambda_1 = 0, \lambda_2 = 5.55, \lambda_{3,4} = -7 \pm 3.16i, \lambda_5 = 10.45$. According to Figure 1, the non-zero eigenvalues locate in the stability region which implies that the underlying network becomes synchronized. Figure 3 shows the underlying network becomes synchronized for this configuration.

In order to simulate the effect of perturbation of interconnection gains on synchronization, we consider a network depicted in Figure 2 (b) in which the interconnection between all nodes are assumed to be same for simplicity. In this case, the Laplacian matrix has five eigenvalues, $\lambda_1 = 0, \lambda_2 = \lambda_3 = \lambda_4 = \lambda_5 = 5K$. Based on our analysis, the underlying network becomes synchronized if $5K \in [5; 15]$. We first set $K = 1.2$. Following the simple case in Remark 3, the interconnection gains between node 1 and node 2 are changed. Condition (42) implies that $|\delta l_{12}| \leq 0.5$, which means the synchronization persists for the range of interconnection for $l_{12} = l_{21} \in [0.7, 1.9]$. On the other hand, conditions (43) and (44) can be used to show that synchronization vanishes for interconnection gains $l_{12} = l_{21} \in [0, 7)$ and $l_{12} = l_{21} \in [8.7, \infty)$. Indeed, these two ranges of values show that the synchronization disappears if the interconnection gain increases or decreases significantly. Figure 4 shows network behavior for the perturbed network when

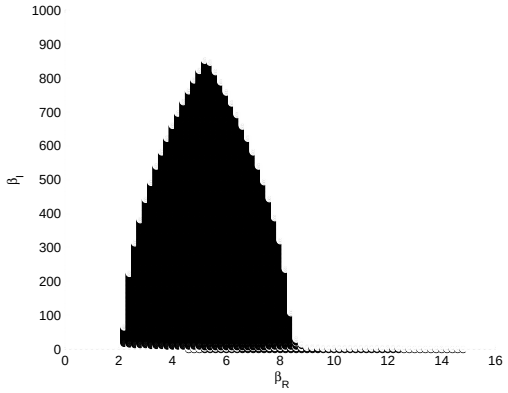

Figure 1: The stability (black) and instability (white) regions of the system (15) with parameters values $a = 10, b = 10, c = 10, d = -2, \rho_x = 2, \rho_y = -6$.

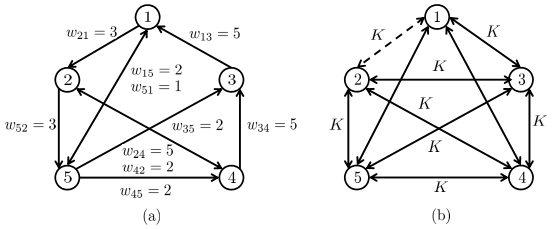

Figure 2: Five diffusively coupled Wilson-Cowan oscillators with (a) directed, (b) undirected interconnection and all to all interconnection with the same gain k. The dotted line indicates the perturbed edges in the network.

the interconnection between nodes 1 and 2 is removed.

This example indicates that the synchronization disappears if the interconnection between two nodes is removed; however, this is not true in general. If the value of $K = 1.8$ is chosen, as depicted in Figure 5, the network becomes synchronized even if the interconnection between nodes 1 and 2 is removed. Indeed, for this choice of K, condition (42) leads to $|\delta l_{12}| \leq 2$, which is larger than the interconnection gain K. This means that, by removing the interconnection between these two nodes, the synchronization may persist. This observations are consistent with the results of [23] that obtained through only simulations.

7. Conclusions

A new procedure has been introduced to analyze synchronization of networks of homogeneous Wilson- Cowan models with diffusive coupling. Using the linearized model around a limit cycle, analytic results have been developed that can be utilized to check for the existence or absence of synchronous behavior. Even though the Wilson-Cowan model does not fit the general model considered in [14; 20], our results can be adopted for that general model. Contrary to [20], we have allowed the interconnection between nodes to be directed. We have proven that the network of Wilson-Cowan models always becomes desynchronized when the Laplacian matrix has some eigenvalues with large real values. A computational approach has been presented for those eigenvalues of the Laplacian matrix with either intermediate values of real part or small values

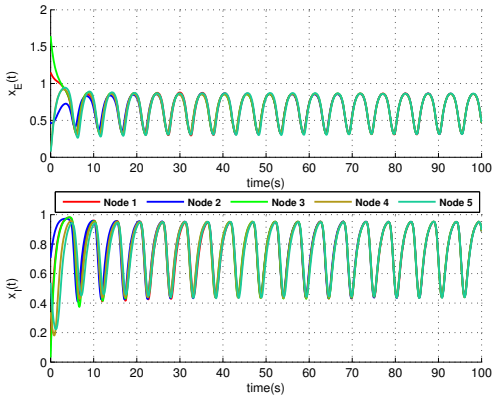

Figure 3: The trajectories of heterogeneous Wilson-Cowan network depicted in Figure 2 (a).

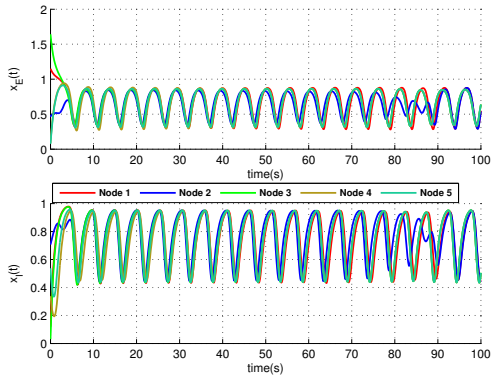

Figure 4: The trajectories of heterogeneous Wilson-Cowan network depicted in Figure 2 (b) and coupling gain $k = 1.2$. The interconnection between nodes 1 and 2 is removed.

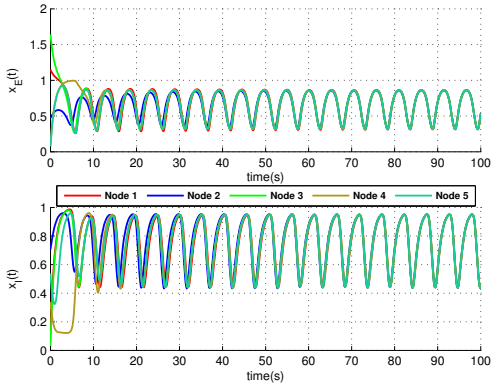

Figure 5: The trajectories of heterogeneous Wilson-Cowan network depicted in Figure 2 (b) and coupling gain $k = 1.8$. The interconnection between nodes 1 and 2 is removed.

of real part and non-small values of imaginary part. We also addressed the presence or absence of synchronous behavior in the case that interconnection gains are perturbed. Simulation results showed the effectiveness of our approach in determining absence or presence of synchronized behavior. As future work, one can study global synchronization in the network of diffusive Wilson-Cowan using the Lipschitz property of the sigmoid function that converts the average membrane potential into an average pulse density of action potentials. Another interesting approach is to extend this method for a homogeneous network and/or for a network with input disturbances at the coupling.

Appendix A.

Proof of Lemma 1. Denote $\beta_{R_k} = \Re(\lambda_k)$ and $\beta_{I_k} = \Im(\lambda_k)$. The structure of Σ_k indicates that the dynamical system (15) consists of m_k subsystems described by,

$$\frac{d}{dt}\begin{bmatrix}\Re(\tilde{y}_{k,i})\\ \Im(\tilde{y}_{k,i})\end{bmatrix} = \begin{bmatrix}\mathcal{A}_{k,1}(t) & \mathcal{A}_{k,2}(t)\\ -\mathcal{A}_{k,2}(t) & \mathcal{A}_{k,1}(t)\end{bmatrix}\begin{bmatrix}\Re(\tilde{y}_{k,i})\\ \Im(\tilde{y}_{k,i})\end{bmatrix} + \tilde{u}_{k,i} \tag{A.1}$$

with $\mathcal{A}_{k,1}(t) = (-\Lambda + A(t)\Xi) - \beta_{R_k}A(t)D$, $\mathcal{A}_{k,2}(t) = \beta_{I_k}A(t)D$, $\hat{u}_{k,m_k} = 0$, and

$$\tilde{u}_{k,i} = \begin{bmatrix}-A(t)D & \mathbf{0}\\ \mathbf{0} & -A(t)D\end{bmatrix}\begin{bmatrix}\Re(\tilde{y}_{k,i+1})\\ \Im(\tilde{y}_{k,i+1})\end{bmatrix}, \tag{A.2}$$

for $i = 1, \ldots, m_k - 1$. From (A.1) and (A.2), it is observed that the system (15) is a cascade structure of m_k identical subsystems where the states of subsystem m_k act as input for the subsystems $m_k - 1$, the states of subsystems $m_k - 1$ are input for the subsystems $m_k - 2$, and so on.

To prove the stability part, we first point out that, for linear periodic systems, asymptotic stability implies uniform asymptotic stability [13, Theorem 7] and exponential stability. If each unforced subsystem is exponentially stable, it is input to state stable (ISS) [12, Lemma 4.6], and so the cascade interconnection of subsystems $i = 1, \ldots, m_k - 1$ is also ISS. Since the subsystem m_k is exponentially stable, the cascade system (15) is uniformly asymptotically stable [12, Lemma 4.7]. It is straightforward to see that the instability of the subsystem m_k leads to instability of the whole system. This completes the proof. □

Lemma 2. *(Instability Using Two-Time Averaging). Consider the linear time-varying system described by the state space model*

$$\begin{aligned}\begin{bmatrix}\dot{\hat{s}}_i\\ \dot{\hat{r}}_i\end{bmatrix} = \left(\begin{bmatrix}\mathbf{0} & \mathbf{0}\\ \mathbf{0} & H\end{bmatrix} - \epsilon\begin{bmatrix}\urcorner_{11}(t) & \urcorner_{12}(t)\\ \urcorner_{21}(t) & \urcorner_{22}(t)\end{bmatrix}\right)\begin{bmatrix}\hat{s}_i\\ \hat{r}_i\end{bmatrix}\\ -(-1)^i\beta\begin{bmatrix}\urcorner_{11}(t) & \urcorner_{12}(t)\\ \urcorner_{21}(t) & \urcorner_{22}(t)\end{bmatrix}\Bigg)\begin{bmatrix}\hat{s}_{3-i}\\ \hat{r}_{3-i}\end{bmatrix}\end{aligned} \tag{A.3}$$

where $\hat{s} \in \mathbb{R}^p$ and $\hat{r} \in \mathbb{R}^q$. Assume that $\urcorner_{ij}(t)$, $i, j = 1, 2$ are T-periodic, piecewise, continuous functions bounded by the scalar $\iota_{ij} > 0$, i.e. $|\urcorner_{ij}(t)| \le \iota_{ij}$ for all $t \ge 0$. Now consider the average system described by

$$\dot{\hat{s}} = -\epsilon\bar{\urcorner}_{11}\hat{s}\ ,\quad \bar{\urcorner}_{11} = \frac{1}{T}\int_0^T \urcorner_{11}(\tau)d\tau. \tag{A.4}$$

If $\bar{\urcorner}_{11}$ and G are Hurwitz, then there exists ϵ^* and $\psi : [0, \epsilon^*] \to \mathbb{R}_{\ge 0}$ such that for every $\epsilon \in (0, \epsilon^*)$ and a corresponding $\beta \in [0, \psi(\epsilon)]$, the origin of system (A.3) is unstable.

Proof. Similar to [19; 20], we change the coordinate of the system by defining a new state $\check{s}$ as

$$\hat{s} \triangleq \mathfrak{H}\check{s} = \left[I - \epsilon\int_0^t (\urcorner_{11}(\tau) - \bar{\urcorner}_{11})d\tau\right]\check{s}. \tag{A.5}$$

Note that since $|\int_0^T (\urcorner_{11}(\tau) - \bar{\urcorner}_{11})d\tau| \le 2T\iota_{11}$, if $\epsilon < \epsilon_1 \triangleq \frac{1}{2T\iota_{11}}$, then the inverse of $\mathfrak{H}$ exists and, therefore, $|\mathfrak{H}^{-1}| \le \gamma = \frac{1}{1-2\epsilon_1 T\iota_{11}}$. In this case, the original system (A.3) is represented in the new coordinates as

$$\begin{aligned}\begin{bmatrix}\dot{\check{s}}_i\\ \dot{\hat{r}}_i\end{bmatrix} = \left(\begin{bmatrix}\mathbf{0} & \mathbf{0}\\ \mathbf{0} & H\end{bmatrix} - \alpha\begin{bmatrix}\mathfrak{M}_{11}(t) & \mathfrak{M}_{12}(t)\\ \mathfrak{M}_{21}(t) & \mathfrak{M}_{22}(t)\end{bmatrix}\right)\begin{bmatrix}\check{s}_i\\ \hat{r}_i\end{bmatrix}\\ -(-1)^i\beta\begin{bmatrix}\mathfrak{Q}_{11}(t) & \mathfrak{Q}_{12}(t)\\ \mathfrak{Q}_{21}(t) & \mathfrak{Q}_{22}(t)\end{bmatrix}\Bigg)\begin{bmatrix}\check{s}_{3-i}\\ \hat{r}_{3-i}\end{bmatrix},\end{aligned} \tag{A.6}$$

where

$$\begin{aligned}&\mathfrak{M}_{11} = \mathfrak{H}^{-1}\urcorner_{11}(t)\mathfrak{H} + \mathfrak{H}^{-1}(\bar{\urcorner}_{11} - \urcorner_{11}(t))\\ &\mathfrak{Q}_{11} = \mathfrak{H}^{-1}\urcorner_{11}(t)\mathfrak{H}\ ,\ \mathfrak{M}_{12} = \mathfrak{Q}_{12} = \mathfrak{H}^{-1}\urcorner_{12}(t)\\ &\mathfrak{M}_{21} = \mathfrak{Q}_{21} = \urcorner_{21}(t)\mathfrak{H}\ ,\ \mathfrak{M}_{22} = \mathfrak{Q}_{22} = \urcorner_{22}(t),\end{aligned} \tag{A.7}$$

Since the matrices $\bar{\urcorner}_{11}$ and G are Hurwitz, there exist positive definite matrices P_s and P_r such that $P_s\bar{\urcorner}_{11} + \bar{\urcorner}_{11}^T P_s = -I$ and $P_r H + H^T P_r = -I$. Now, define the Lyapunov function as $V = \sum_{i=1}^{2} \check{s}_i^T P_s\check{s}_i - \hat{r}_i^T P_r\hat{r}_i$. Taking the derivative of the Lyapunov function leads to

$$\begin{aligned}\dot{V} \ge&(\epsilon\gamma - 4T\epsilon^2\gamma\iota_{11}^2|P_s|)|\check{s}_1|^2 - 4\epsilon\gamma\iota_{12}|P_r||\check{s}_1||\hat{r}_1|\\ &+ (1 - 2\epsilon\iota_{22}|P_r|)|\hat{r}_1|^2 - 2\epsilon\iota_{21}(1 + 2\epsilon T\iota_{11})|P_r||\hat{r}_1||\check{s}_1|\\ &(\epsilon\gamma - 4T\epsilon^2\gamma\iota_{11}^2|P_s|)|\check{s}_2|^2 - 4\epsilon\gamma\iota_{12}|P_r||\check{s}_2||\hat{r}_2|\\ &+ (1 - 2\epsilon\iota_{22}|P_r|)|\hat{r}_2|^2 - 2\epsilon\iota_{21}(1 + 2\epsilon T\iota_{11})|P_r||\hat{r}_2||\check{s}_2|\\ &+ \beta\left(2\check{s}_1^T P_s(\mathfrak{Q}_{11}\check{s}_2 + \mathfrak{Q}_{12}\hat{r}_2) - 2\hat{r}_1^T P_r(\mathfrak{Q}_{21}\check{s}_2 + \mathfrak{Q}_{22}\hat{r}_2)\right)\\ &+ \beta\left(-2\check{s}_2^T P_s(\mathfrak{Q}_{11}\check{s}_1 + \mathfrak{Q}_{12}\hat{r}_1) + 2\hat{r}_2^T P_r(\mathfrak{Q}_{21}\check{s}_1 + \mathfrak{Q}_{22}\hat{r}_1)\right).\end{aligned} \tag{A.8}$$

If $\epsilon \le \frac{\epsilon_1}{2|P_s|}$ and $\epsilon \le \epsilon_2 \triangleq \frac{1}{\iota_{22}|P_r|}$, the first, third, fifth, and seventh terms of (A.8) are positive, and, hence there exists ϵ such that the derivative of the Lyapunov function is positive when $\beta = 0$. Indeed, using the Schur complement, the positiveness of the right hand side of (A.8) in the case of $\beta = 0$ is equivalent to existence of positive value ϵ_3 such that $\mathcal{F} = \begin{bmatrix}\digamma_{11} & \digamma_{12}\\ \digamma_{12} & \digamma_{22}\end{bmatrix} > 0$ with $\digamma_{11} = \epsilon_3\gamma - 4T\epsilon_3^2\gamma\iota_{11}^2|P_w|$, $\digamma_{22} = 1 - 2\epsilon_3\iota_{22}|P_r|$, and $\digamma_{12} = -(\epsilon_3\gamma\iota_{12}|P_s| + \epsilon_3\iota_{21}(1 + 2\epsilon T\iota_{11})|P_r|)$. Now, let us define $\epsilon^* \triangleq \min(\epsilon_1, \frac{\epsilon_1}{2|P_s|}\epsilon_2, \epsilon_3)$. Then, for every $\epsilon \in (0, \epsilon^*)$, the inverse of the coordinate change exists and the derivative of the Lyapunov function is positive when $\beta = 0$. Now, pick any $\bar{\epsilon} \in (0, \epsilon^*)$ and denote the evaluated matrix $\mathcal{F}$ at $\bar{\epsilon}$ by $\bar{\mathcal{F}}$. We obtain the associated $\psi(\bar{\epsilon})$ by solving the following optimization problem:

$$\psi(\bar{\epsilon}) = \max_{\bar{\beta}>0}\bar{\beta} \qquad s.t. \quad \begin{bmatrix}\bar{\mathcal{F}} & \bar{\beta}\bar{\mathcal{Z}}\\ \bar{\beta}\bar{\mathcal{Z}} & \bar{\mathcal{F}}\end{bmatrix} < 0, \tag{A.9}$$

where $\bar{\mathcal{Z}} = \begin{bmatrix} 2|P_s|\gamma\iota_{11}(1+2T\bar{\epsilon}\iota_{11}) & 2|P_s|\gamma\iota_{12} \\ 2|P_r|(1+2T\bar{\epsilon}\iota_{11})\iota_{21} & 2|P_r|\iota_{22} \end{bmatrix}$. Under this set up, $\dot{V} > 0$ for $\bar{\epsilon}$ and $\beta \in [0, \psi(\bar{\epsilon})]$. Note that the set $\Omega \triangleq \{(\check{s}_1, \hat{r}_1, \check{s}_2, \hat{r}_2) \in \mathbb{R}^{2(p+q)} \mid V \geq 0\}$ is nonempty, since the candidate Lyapunov function is quadratic type. Hence, according to Chetaev's theorem for time-varying systems [10], the origin of (A.3) is unstable. This completes the proof. □

Remark 4. *In the proof of Lemma 2, it is straightforward to check that if $P_s\mathfrak{Q}_{11} = \mathfrak{Q}_{11}^T P_s$ and $P_r\mathfrak{Q}_{22} = \mathfrak{Q}_{22}^T P_r$, then the matrix $\bar{\mathcal{Z}}$ is simplified to*

$$\bar{\mathcal{Z}} = \begin{bmatrix} 0 & 2|P_s|\gamma\iota_{12} \\ 2|P_r|(1+2T\bar{\epsilon}\iota_{11})\iota_{21} & 0 \end{bmatrix},$$

which leads to a less conservative result.

References

[1] Agaev, R., Chebotarev, P., 2005. On the spectra of nonsymmetric laplacian matrices. Linear Algebra and its Applications 399, 157–168.

[2] Ahmadizadeh, S., Nešić, D., Freestone, R. D., Grayden, D. B., 2015. Analytic synchronization conditions for a network of Wilson and Cowan oscillators. In: 54th Annual Conference on Decision and Control (CDC). IEEE, pp. 3104–3109.

[3] Arcak, M., 2010. Passivity Approach to Network Stability Analysis and Distributed Control Synthesis. The Control Systems Handbook, Second Edition.

[4] Belykh, I., Belykh, V., Hasler, M., 2006. Generalized connection graph method for synchronization in asymmetrical networks. Physica D: Nonlinear Phenomena 224 (1), 42–51.

[5] Bernstein, D. S., 2009. Matrix Mathematics: Theory, Facts, and Formulas. Princeton University Press.

[6] Daffertshofer, A., van Wijk, B. C., 2011. On the influence of amplitude on the connectivity between phases. Frontiers in Neuroinformatics 5.

[7] DeLellis, P., di Bernardo, M., Russo, G., 2011. On QUAD, lipschitz, and contracting vector fields for consensus and synchronization of networks. IEEE Transactions on Circuits and Systems I: Regular Papers 58 (3), 576–583.

[8] Demir, A., Mehrotra, A., Roychowdhury, J., 2000. Phase noise in oscillators: a unifying theory and numerical methods for characterization. IEEE Transactions on Circuits and Systems I: Fundamental Theory and Applications 47 (5), 655–674.

[9] Farkas, M., 1994. Periodic Motions. Springer-Verlag.

[10] Haddad, W. M., Chellaboina, V., 2008. Nonlinear Dynamical Systems and Control: a Lyapunov-based Approach. Princeton University Press.

[11] Hoppensteadt, F. C., Izhikevich, E. M., 1997. Weakly Connected Neural Networks. Vol. 126. Springer New York.

[12] Khalil, H. K., 2002. Nonlinear Systems, 3rd Edition.

[13] Massera, J. L., 1956. Contributions to stability theory. Annals of Mathematics, 182–206.

[14] Pecora, L. M., Carroll, T. L., 1998. Master stability functions for synchronized coupled systems. Physical Review Letters 80 (10), 2109.

[15] Porfiri, M., Di Bernardo, M., 2008. Criteria for global pinning-controllability of complex networks. Automatica 44 (12), 3100–3106.

[16] Ren, W., Beard, R. W., 2005. Consensus seeking in multiagent systems under dynamically changing interaction topologies. IEEE Transactions on Automatic Control 50 (5), 655–661.

[17] Rodriguez, E., George, N., Lachaux, J.-P., Martinerie, J., Renault, B., Varela, F. J., 1999. Perception's shadow: long-distance synchronization of human brain activity. Nature 397 (6718), 430–433.

[18] Sandberg, H., Mollerstedt, E., Bernhardsson, B., 2005. Frequency-domain analysis of linear time-periodic systems. IEEE Transactions on Automatic Control 50 (12), 1971–1983.

[19] Sastry, S., Bodson, M., 2011. Adaptive Control: Stability, Convergence and Robustness. Courier Corporation.

[20] Shafi, S. Y., Arcak, M., Jovanović, M., Packard, A. K., 2013. Synchronization of diffusively-coupled limit cycle oscillators. Automatica 49 (12), 3613–3622.

[21] Stan, G.-B., Sepulchre, R., 2007. Analysis of interconnected oscillators by dissipativity theory. IEEE Transactions on Automatic Control 52 (2), 256–270.

[22] Steur, E., Tyukin, I., Nijmeijer, H., 2009. Semi-passivity and synchronization of diffusively coupled neuronal oscillators. Physica D: Nonlinear Phenomena 238 (21), 2119–2128.

[23] Terry, J. R., Benjamin, O., Richardson, M. P., 2012. Seizure generation: the role of nodes and networks. Epilepsia 53 (9), e166–e169.

[24] Ueta, T., Chen, G., 2003. On synchronization and control of coupled Wilson-Cowan neural oscillators. International Journal of Bifurcation and Chaos 13 (01), 163–175.

[25] Wilson, H. R., Cowan, J. D., 1972. Excitatory and inhibitory interactions in localized populations of model neurons. Biophysical Journal 12 (1), 1–24.

[26] Yu, W., Chen, G., Cao, M., 2011. Consensus in directed networks of agents with nonlinear dynamics. IEEE Transactions on Automatic Control 56 (6), 1436–1441.

[27] Zhou, J., Hagiwara, T., 2005. 2-regularized Nyquist criterion in linear continuous-time periodic systems and its implementation. SIAM Journal on Control and Optimization 44 (2), 618–645.